Acta Geologica Sinica (English Edition), 2019, 93(1): 155–166

Sedimentary Evolution and Transgressions of the Western Subei Basin in Eastern China since the Late Pliocene

CHENG Yu[1,*], LI Xiangqian[1], SHU Junwu[2], BAI Shibiao[3], ZHAO Zengyu[1], ZHANG Xiangyun[1], GUO Gang[1], ZHANG Ping[1] and LIN Jingxing[4]

[1] *The Institute of Geological Survey of Jiangsu Province, Nanjing 210018, Jiangsu, China*
[2] *Nanjing Institute of Geology and Palaeontology, CAS Key Laboratory of Economic Stratigraphy and Palaeogeography, Chinese Academy of Sciences, Nanjing 210008, Jiangsu, China*
[3] *School of Geography Science, Nanjing Normal University, Nanjing 210023, Jiangsu, China*
[4] *Institute of Geology, Chinese Academy of Geological Sciences, Beijing 100037, China*

Abstract: Sedimentary sequences in the Subei Basin are complex and have been affected by interactions between the ocean and rivers since the Late Pliocene, including the Yellow River, Huaihe River, and the Yangtze River. This sedimentary evolution, in particular the timing of Pleistocene transgressions, has long been a matter of controversy owing to the lack of precise chronological evidence. The aim of this study is to explore the evolution of the sedimentary environment throughout the past 3.00 Ma in this region on the basis of a comprehensive analysis of particle size and foraminifera and ostracods collected in the TZK9 core from the Subei Basin combined with geochronological studies of magnetostratigraphy, AMS^{14}C and optically stimulated luminescence (OSL). The results show that fluvial facies in the sedimentary environment from 3.00 to 1.01 Ma. There were fluvial facies and reflects six sea-level high stands from 1.01 to 0.25 Ma. The study area was affected by four large-scale transgressions since 0.25 Ma. The four marine sedimentary layers known as DU7 (buried at 48–52 m), DU5 (buried at 35–41 m), DU3 (buried at 16–23 m), and DU1 (buried at 2–4 m) are recorded in the MIS7 (210–250 ka), MIS5, MIS3, and Holocene, respectively. The magnitude of the DU5 transgression was identical to that of the DU3 transgression, both were larger than the DU7 transgression, and the DU1 transgression was the weakest. The variation of transgression strength reflects the influence of global changes in sea level, tectonic subsidence, shell ridges, and sand dams. In the TZK9 core, we found evidence of seven sea-level high stands from the Early–Middle Pleistocene, and the first one caused by regional rapid subsidence and could be traced back to 0.83-0.84 Ma. The sea-level high stands and the age of the first one recorded above was different from other cores in eastern China, this was caused by the lack of absolute age control and the differences in paleotopography during this period. This study reconstructs sedimentary evolution, determines the transgression and its age, establishes the chronology since the Late Pliocene, and provides a scientific framework for further paleoenvironmental and tectonic studies. The results of this study highlight the important role that local tectonics and global sea level play in the sedimentary evolution and transgressions that have occurred in the western Subei Basin.

Key words: foraminifera and ostracods, sea-level change, transgression, Subei Basin

Citation: Cheng et al., 2019. Sedimentary Evolution and Transgressions of the Western Subei Basin in Eastern China since the Late Pliocene. *Acta Geologica Sinica* (English Edition), 93(1): 155–166. DOI: 10.1111/1755-6724.13645

1 Introduction

Since the 1970s, in eastern China, scientific campaigns have drilled multiple boreholes to understand transgression events that took place in the Quaternary (Lin Jingxing, 1977; Zhao Songling et al., 1978; Wang Pinxian et al., 1981; Wang Qiang and Li Fenglin, 1983; Wu Biaoyun and Li Congxian, 1987; Lin et al., 1989; Yang Zhigeng, 1993). Previous studies have discovered five to eight transgression events in the Quaternary and three in the Late Quaternary (Wang Pinxian et al., 1981; Wu Biaoyun and Li Congxian, 1987; Wang Zhanghua et al., 2004, 2008; Liu et al., 2009, 2010; Lin et al., 2012; Wang et al., 2013; Li Shoujun et al., 2017; Yu Zhangxin et al., 2017). With the application of AMS^{14}C and optically stimulated luminescence (OSL) dating, previous studies have preliminarily identified the age of the three transgressions from the Late Quaternary: the MIS5 (the third transgressive layer), the MIS3 (the second transgressive layer), and the Holocene (MIS1) (the first sea invasion) (Zhao Songling et al., 1978; Liu et al., 2009, 2016b; Wang et al., 2013; Shang Zhiwen et al., 2015). It has been proposed in previous studies that the depth of the B/M boundary is greater than 150 m in eastern China, which yielded estimated transgression ages of 150 ka (the fourth sea invasion layer), 300 ka (the fifth transgressive layer), and 2.3 Ma (the sixth transgressive layer) (Wang Pinxian et al., 1981; Wang Qiang et al., 1986; Wu Biaoyun and Li Congxian, 1987). Most of the literature cited above contained analyzes of the magnetic

* Corresponding author. E-mail: ftchengyu@msn.com

http://www.geojournals.cn/dzxbcn/ch/index.aspx
https://onlinelibrary.wiley.com/journal/17556724

stratigraphy using alternating demagnetization at a low sampling density. With the wide application of thermal demagnetization in river and lake sediments and the increases in the sampling density, results from continuous and high-resolution magnetic stratigraphy have moved the B/M boundary to a depth of 70–100 m in eastern China, which corresponds to the Subei Basin (Cheng Yu et al., 2016), the South Yellow Sea (Ge Shulan et al., 2005; Liu et al., 2014a, 2014b; Mei et al., 2016), the Bohai Basin (Yao et al., 2014; Li Xiang et al., 2016; Liu et al., 2016a), and the Yangtze River Delta (Duan et al., 2015, Cheng Yu et al., 2018b).

Based on the identification and definition of transgressive layers, evidence from deep-sea oxygen isotope curves shows that Early Pleistocene and Middle Pleistocene marine strata are consistent with an interglacial period (Li Xiaoyan et al., 2015). However, transgressive chronologies are focused mainly in the South Yellow Sea and the regions adjacent to the Bohai during the Quaternary (Shi Linfeng et al., 2009; Yi et al., 2012; Liu et al., 2016a, 2016b). Mentions of the Subei Basin are scarce in the literature (Yang Jinghong et al., 2006; Zhang Zhenke et al., 2010). Chen Wanli et al. (1998) identified five separate marine transgressions since the Early Pleistocene on the basis of analyses of micropaleontology, paleomagnetism, and sporopollen. Based on the analysis of multiple indices in the BY1 core, Yang Jinghong et al. (2006) identified four transgressions in the Subei Basin. However, transgressions and, by extension, their age are still not well understood in the Subei Basin owing to the lack of a reliable chronological framework. The Subei Basin is not only an important region in the East Asian monsoon climate, but also a key area that connects the sea to farther inland area. This basin is a suitable region to study sedimentary evolution during the Quaternary owing to the stable subsidence rate, continuous stratigraphy, and numerous transgressions (Chen Wanli et al., 1998; Shu Qiang et al., 2006; Yang Jinghong et al., 2006; Zhang Maoheng, 2009; Zhang Zheke et al., 2010).

Based on the analysis of sedimentary characteristics, grain size, foraminifera, and ostracods from the TZK9 core, this study aims to establish a sedimentary history of the western Subei Basin since the Late Pliocene by focusing mainly on the transgressions and their ages.

2 Geological Setting

The Subei Basin lies between 32°10′ and 35°05′ N and between 118°40′ and 120°30′ E to the northeast of the Yangtze Block (Fig. 1). The basin is adjacent to the Tancheng-Lujiang Fault in the west, the Yellow Sea in the east, the Sulu Orogenic Belt in the north, and the Tongyang Uplift in the south. Due to the subduction of the Pacific Plate beneath the East Asian Plate in the Late Cretaceous–Paleogene, two depressions and one uplift formed (i.e., the Yanfu Depression, the Dongtai Depression, and the Jianhu Uplift) (Duan Liu'an et al., 2017). The Subei Basin has significantly subsided because of the rise of the Tibetan Plateau since the Neogene (Pang Yumao et al., 2017; Mei Mingxiang and Liu Shaofeng, 2017). The basin has deposited thousands of fluvial and

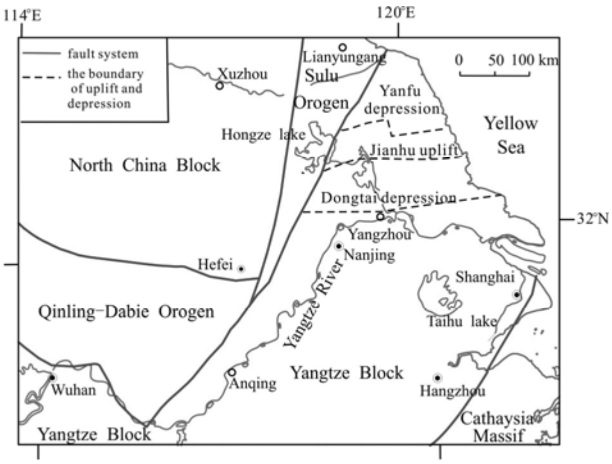

Fig. 1. Map showing the main depositional basins, faults, and areas of uplift in eastern China.

lacustrine strata, which have gradually flattened and developed into a plain environment owing to interactions between rivers, oceans, and lakes (Wang Ying et al., 2006; Yang Jinghong et al., 2007).

The sediment lithology is characterized by yellow to brown-yellow clay and silty clay. Gray sandy gravel layers are also found since the Late Pliocene. During the interglacial period, when the sea level rose faster than the sediment accumulation rate, the seawater infiltrated the Subei Basin and preserved a large number of micropaleontological fossils.

3 Samples and Methods

The TZK9 core (32°35′ N, 120°06′ E, ground elevation: 2 m), shown in Fig. 2, is located approximately 20 km northeast of the city of Taizhou in the province of Jiangsu, China. The Institute of Geological Survey of Jiangsu Province drilled the core in 2015. The depth of drilling was 286.86 m, which yielded a core length of 278.68 m. Core recovery was 97.10%. The lithology is composed of yellow to brown-yellow clay and silty clay. The thick yellowish-brown clay is the dominant sediment in the TZK9 core from 134.00 to 286.86 m and contains calcareous nodules and Fe-Mn nodules. The core also contains gray sandy gravels in the 134.60–144.10 m, 171.50–183.50 m, and 245.90–267.80 m intervals. The lithology from 0 to 134.00 m in the core contains gray and gray-yellow clay, silty clay, and silt, of which several stratigraphic layers developed horizontal bedding due to tidal action.

AMS^{14}C dating of the TZK9 core was obtained from organic matter that was tested from three samples (Table 1) at Beta Analytic Inc. (Miami, FL, USA). The calendar age was calibrated using the calib7.1 software (Stuiver and Reimer, 1986–2014). In this study, the calibrated ages are reported as calendar ^{14}C ages before AD 1950 (cal a BP), with the uncertainty reported as two standard deviations (2σ) and uncalibrated ages given as ^{14}C years BP (^{14}C a BP) (Table 1).

The sediment grain sizes of 359 samples at the 50–100 cm interval were tested using the standard treatment

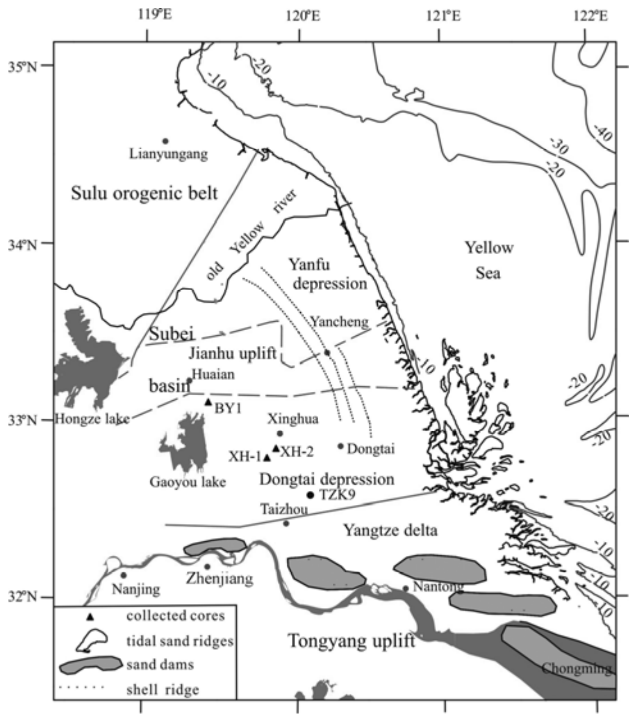

Fig. 2. Map showing the locations of the cores used in this study of the Subei Basin

Cores BY1, XH-1, and XH-2 are from Yang Jinghong et al. (2007), Shu Qiang (2004), and Zhang Zhenke (2009), respectively.

method (Lu et al., 1997; Lu Huayu et al., 2002) at the laboratory of the Institute of Geochemistry, Chinese Academy of Sciences, using the Malvern Mastersizer 2000.

Microfossil analysis (including benthic foraminifera and ostracods), mainly at 0.5–2.0 m intervals, was performed on 165 samples from all sedimentary layers and analyzed by the standard treatment method described by Wang Pinxian et al. (1988). All samples were identified at the Institute of Geology, Chinese Academy of Geological Sciences.

Paleomagnetism analysis was performed at the State Key Laboratory for Mineral Deposit Research, Nanjing University. Based on the various lithologies, 382 samples, at intervals between 0.3 and 0.6 m, were thermally demagnetized at a temperature range of 15–100°C with an MMTD80 automatic thermal demagnetizer. The natural remnant magnetization of all samples was tested before thermal demagnetization. The sample demagnetization effect was ideal, and the magnetostratigraphy of the core has been previously published (Cheng Yu et al., 2016).

Three samples, within 40 m of each other, were collected for OSL analysis at the School of Geographical Science, Nanjing Normal University. A single-aliquot regenerative dose protocol was used during the OSL measurements. The results of the OSL analyses are based on the quartz signal and are listed in Table 2.

4 Results

The abundance of foraminifera and ostracods in the TZK9 core varied between 0 and 831 pieces/50 g and between 0 and 21 pieces/50 g, respectively, since the Late Pliocene. Sample diversity in the foraminifera ranged from 1 to 9. The main species of foraminifera is the *Ammonia beccarii/tepida* Group, which lives in warm water at depths between 0 and 20 m (Wang Pinxian et al., 1985, 1988). The foraminifera contain a small amount of *Elphidium advenum*, which is a coastal species that is distributed at depths between 20 and 50 m. In addition, *Cribrononion incertum*, *Elphidium* spp., *Elphidiella kiangsuensis*, *Bolivina* sp., *Pseudononionella variabilis*, and *Stomoloculina multangula* were also found in the core. The ostracods are mainly *Ilyocypris* sp., *Ilyocypris bradyi*, and *Candoniella albicans*, all of which live in warm freshwater and brackish water (Zhang Hucai et al., 2008; Li Shoujun et al., 2016).

The median grain size, the mean value, the mean square deviation (MSD), skewness, and kurtosis (Friedman, 1978) were used to understand the changes in grain size and hydrodynamic conditions. We divided the sediment in the TZK9 core into nine units on the basis of depositional features (Fig. 3), grain size characteristics (Fig. 4), and the distributions of foraminifera and ostracod assemblages from the base to the top of the core (Fig. 5).

DU9 (286.86–134.00 m) is mainly composed of fine-grained clay (Fig. 3r) and coarse-grained gravel layers (Fig. 3q). The clay is predominately grayish yellow and grayish green in color and contains both caliche and Fe-Mn nodules in certain layers. Erosional basal boundaries exist between the sandy gravel and clay.

The mean value, median grain size, MSD, skewness, and kurtosis were 71.77 μm, 53.31 μm, 1.80 (Φ), 0.62, and 0.21, respectively, which indicate that the hydrodynamic conditions significantly changed. The main sandy gravel layers developed along the intervals of 134.60–144.10 m, 171.50–183.50 m, and 245.90–267.80 m. The mean value, median grain size, MSD, skewness, and kurtosis of the sandy gravel were 175.48 μm, 140.33 μm, 2.13 (Φ), 1.14, and 0.95, respectively, which all indicate that the hydrodynamic power was quite strong.

There are no occurrences of foraminifera in this unit. *Chara* spores, which occur at 184.60 m, may be transported by wind and water flow. Found in several layers, terrestrial ostracods, which mainly include *Candoniella albicans*, *Ilyocypris* sp., and *Ilyocypris bradyi*, have a sample diversity of 1–3. Therefore, we interpreted this unit as a fluvial environment, such as a floodplain characterized by weak water power or riverbeds characterized by strong hydrodynamic forces.

DU8–DU1 (134.00–0 m).

With an average of 16.70 μm, the median grain size

Table 1 AMS^{14}C ages from the TZK9 core

Depth (m)	Material	$\delta^{13}C$ (‰)	AMS^{14}C age (a BP)	Calibrated age (2σ) (cal a BP)
10.90	Organic matter	−25.5	21500±70	25807±159
12.50	Organic matter	−27.1	34340±260	38919±578
14.50	Organic matter	−27.8	26070±110	30329.5±416

Table 2 OSL dating results for the TZK9 core

Depth (m)	Water (%)	K (%)	Th (ppm)	U (ppm)	De (Gy)	Age (ka)
26.20–26.40	21.68	1.71	12.9	2.36	405.29	153.65±16.56
32.70–32.90	27.81	2.18	13.7	2.36	438.26	158.48±12.89
39.00–39.20	28.78	2.14	11.8	2.39	431.84	166.58±14.14

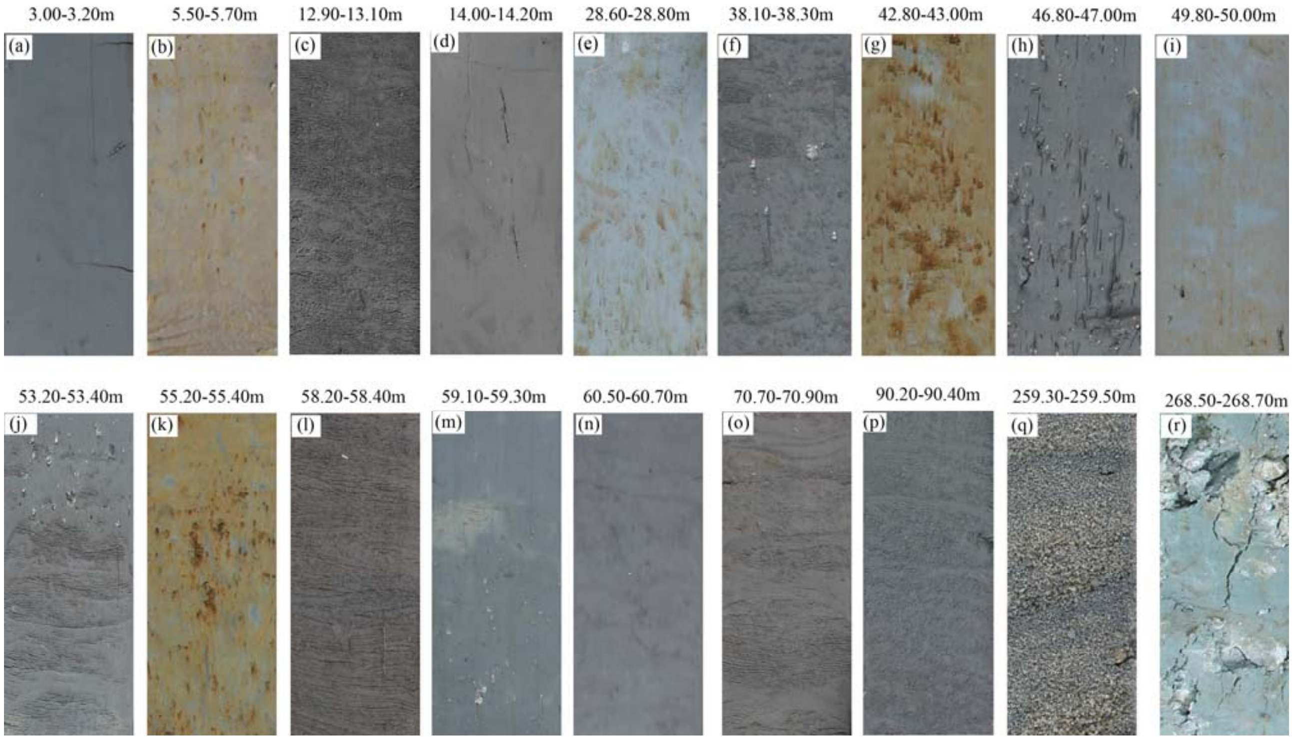

Fig. 3. Photographs of the representative sedimentary facies of the TZK9 core.
(a) 3.00–3.20 m (DU1): gray, grayish-black clay. (b) 5.50–5.70 m (DU2): grayish-yellow silty clay. (c) 12.90–13.10 m (DU3): gray clay and clayey silt, which are characterized by horizontal bedding together with the silt–clay couplet. (d) 14.00–14.20 m (DU3): gray and grayish-black clay. (e) 28.60–28.80 m (DU4): gray and grayish-green clay and clayey silt. (f) 38.10–38.30 m (DU5): gray and brownish-yellow clay, clayey silt, which is characterized by horizontal bedding. (g) 42.80–43.00 m (DU6): gray and silty clay, which contains rusty-yellow Fe-Mn nodules. (h) 46.80–47.00 m (DU7): dark-gray clay, which contains an abundance of shells and shell fragments. DU8 (face A): (j) 53.20–53.40 m, (l) 58.20–58.40 m, (n) 60.50–60.70 m, and (o) 70.70–70.90 m, (p) 90.20-90.40 m, gray and grayish-black clay, which is characterized by horizontal bedding together with clay–silt couplets. DU8 (face B): (i) 49.80–50.00 m, (k) 55.20–55.40 m, (m) 59.10–59.30 m, yellow and grayish-green clay, which contains rusty-yellow Fe-Mn nodules. (q) 259.30–259.50 m (DU9): sandy gravel layers. (r) 268.50–268.70 m (DU9): grayish-green clay.

from 0–134.00 m varies from 6.30 to 50.00 μm. The mean value, MSD, skewness, and kurtosis are 28.86 μm, 1.67 (Φ), 0.52, and 0.09, respectively, which indicates that the hydrodynamic conditions were weak and the depositional environment was stable. We interpret this unit as a floodplain, lacustrine, or marine facies environment with weak hydrodynamic conditions.

(1) DU8 (134.00–48.20 m). This unit consists of two types of sedimentary facies: A and B. Facies A developed horizontal bedding with clay and silt from 90.20–91.90 m (Fig. 3p), 70.50–71.10 m (Fig. 3o), 64.80, 60.30–61.20 m (Fig. 3n), 57.05–58.50 m (Fig. 3l), and 51.80–53.70 m (Fig. 3j). The sediment contains foraminifera, fossil tubes, shell fragments, and shell sands from adjacent areas, which indicates proximity to the coastline and formation in a sea-level high stand. Facies B is mainly composed of grayish-yellow and grayish-green clay (Figs. 3k, 3m, and 3i), which contain continental ostracods in several layers. Continental ostracods, which consist of *Candoniella albicans*, *Ilyocypris* sp., and *Ilyocypris bradyi*, have very low abundances (0–12 pieces/50 g) and low diversities (0–3). These characteristics indicate that the sedimentary environment of facies B was a floodplain.

(2) DU7 (48.20–45.50 m). This unit is characterized by dark-gray clay and contains abundant marine ostracods and shellfish (Fig. 3h). The median grain size ranges from 8.00 to 14.00 μm. A small number of foraminifera observed in this unit, which are dominated by the *Ammonia beccarii/tepida* Group, have lower abundances (1–44 pieces/50 g) and lower diversities (1–3), which we interpret as a lagoon environment.

(3) DU6 (45.50–40.40 m). This unit consists of gray and silty clay (Fig. 3g) and contains rusty-yellow Fe-Mn nodules. The median grain size ranges from 16.00 to 30.00 μm. This unit is completely devoid of foraminifera and ostracods and is interpreted as terrestrial deposition.

(4) DU5 (40.40–29.00 m). The sediment of this unit consists of gray and brownish-yellow clay and clayey silt (Fig. 3f) with horizontal bedding. The median grain size varies between 9.00 and 28.00 μm, which indicates that the hydrodynamic conditions were weak. A large number of marine shellfish, continental ostracods (*Ilyocypris* sp.

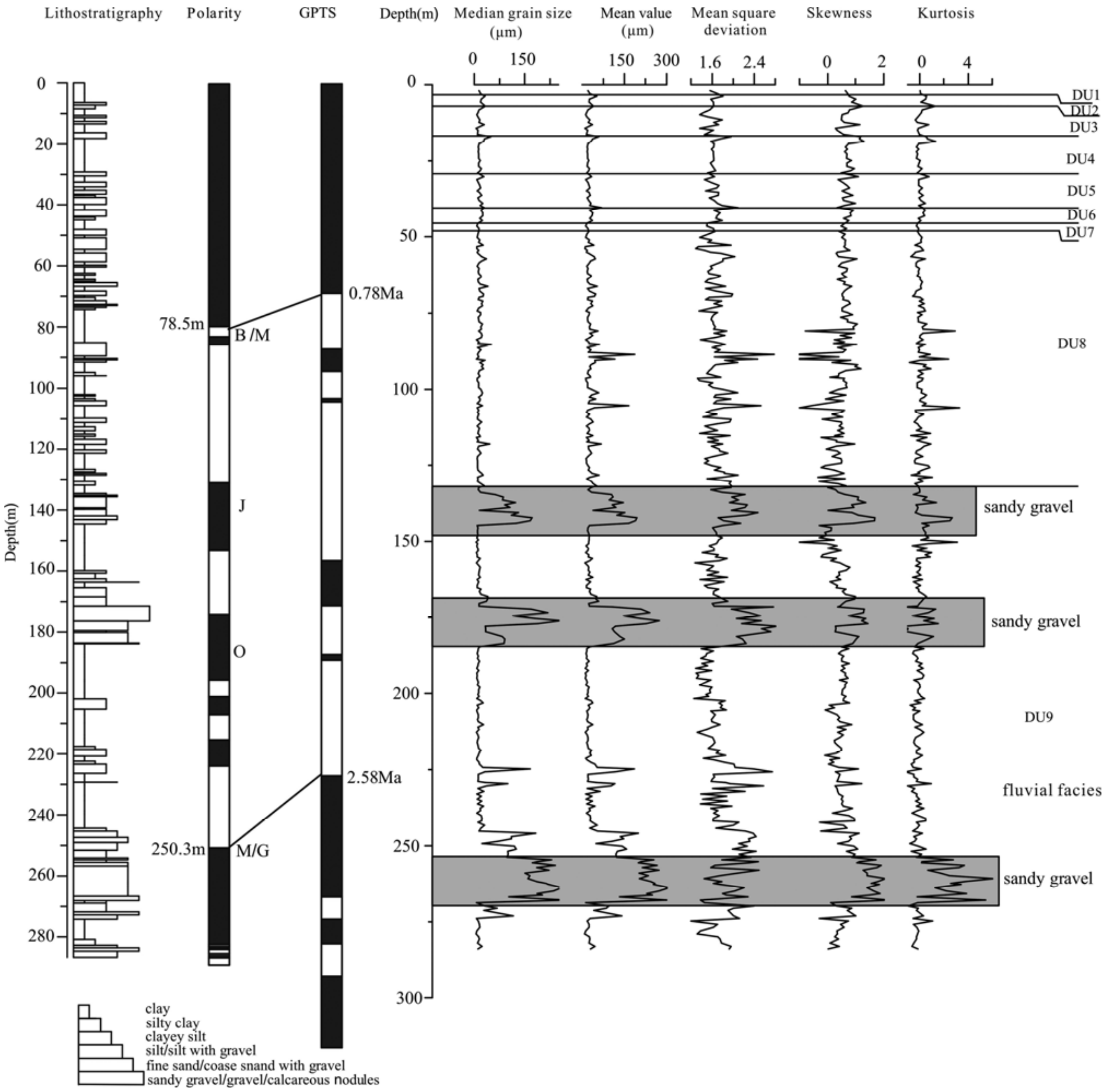

Fig. 4. Variations in the lithostratigraphy, polarity, median grain size, mean value, MSD, skewness, and kurtosis in the TZK9 core.

and *Ilyocypris bradyi*), and foraminifera were observed throughout the unit. Foraminifera, which are dominated by the *Ammonia beccarii/tepida* Group, have an abundance of 25–423 pieces/50 g and a sample diversity of 4–8. A small number of brackish species, such as *Noniron* sp., *Elphidium advenum*, *Elphidiella kiangsuensis*, *Elphidium* sp., and *Nonion tisburyensis*, were also found. These characteristics indicate that the climate was warm and humid and that the sedimentary environment was either at a supralittoral or at an intertidal zone.

(5) DU4 (29.00–16.90 m). This unit has a median grain size ranging from 10.00 to 31.00 μm and consists of gray and grayish-green clay, clayey silt, and calcareous tuberculosis (Fig. 3e). However, no foraminifera were found in this unit, which indicates that the sedimentary environment was terrestrial.

(6) DU3 (16.90–7.00 m). This unit consists of gray clay and clayey silt with horizontal bedding (Figs. 3c and 3d), and the median grain size varies between 6.00 and 50.00 μm. A large number of foraminifera, marine shellfish, marine ostracods, scolite, and terrestrial ostracods (*Ilyocypris* sp. and *Ilyocypris bradyi*) were observed in this unit. The foraminifera mainly consist of the *Ammonia beccarii/tepida* Group with an abundance of 1–831 pieces/50 g and a sample diversity of 1–9. A large number of coastal species, such as *Nonion tisburyensis*, and brackish species, such as *Elphidium advenum*, *Elphidiella kiangsuensis*, *Pseudononionella variabilis*, and *Stomoloculina multangula*, were also found. These characteristics suggest that the climate was warm and

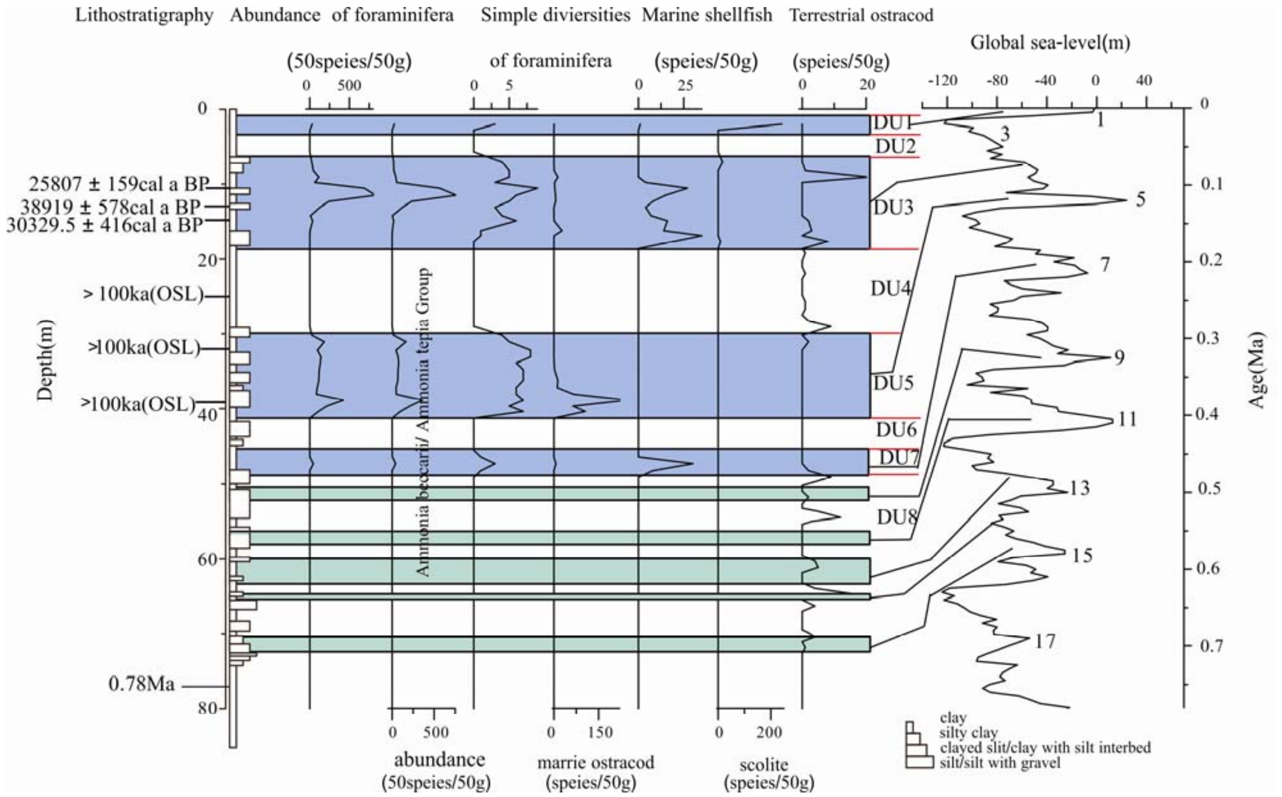

Fig. 5. Downcore changes in foraminiferal abundance, sample diversity, marine shellfish, and terrestrial ostracods in the upper 78 m of the TZK9 core.
The blue shading indicates the four major marine sedimentary beds. The green shading represents a period of sea-level high stand.

humid and that the sedimentary environment was a supralittoral or an intertidal zone.

(7) DU2 (7.00–3.33 m). This unit consists of grayish-yellow silty clay (Fig. 3b), and the median grain size varies between 18.00 and 33.00 μm. No foraminifera or ostracods were found in this unit, which indicates that the sedimentary environment was terrestrial.

(8) DU1 (3.33–0.00 m). This unit is mainly composed of gray and grayish-black clay [Fig 3a], with a median grain size that varies between 14.00 and 19.00 μm, and contains a small number of marine ostracods, marine shellfish, scolite, and foraminifera, which are dominated by the *Ammonia beccarii/tepida* Group, with an abundance of 0–29 pieces/50 g and a sample diversity of 3. These characteristics indicate that the sedimentary environment was a lagoon.

5 Discussions

5.1 Chronostratigraphic Framework of the Core

Using the magnetostratigraphic results, together with the OSL and AMS^{14}C dating results, we were able to establish a chronostratigraphic framework for the sedimentary sequence of the TZK9 core (Figs. 4 and 6; Cheng Yu et al., 2016). The magnetostratigraphic results show that the M/G and B/M layers occur at depths of 250.30 and 78.50 m, respectively. Extrapolation using the accumulation rates suggests that the basal age for the sediment in this core is approximately 3.00 Ma. Jaramillo and Olduvai are located at 129.00–150.20 m and 172.55–192.80 m, respectively. We estimated an age of approximately 1.01 Ma (134.00 m) by interpolation on the basis of the average sedimentation rate in the core section between the upper boundary of Jaramillo (129.00 m, 0.99 Ma; Gradstein et al., 2012) and the basal boundary of Jaramillo (150.20 m, 1.07 Ma; Gradstein et al., 2012). We estimated an age of 0.83–0.84 Ma (90.20–91.90 m) by interpolation on the basis of the average sedimentation rate in the core section between the B/M boundary (78.50 m, 0.781 Ma; Gradstein et al., 2012) and the upper boundary of Jaramillo (129.00 m, 0.99 Ma; Gradstein et al., 2012). Similarly, the corresponding ages for the 134.60–144.10 m, 171.50–183.50 m, and 245.90–267.80 m sections are 1.01–1.04 Ma, 1.77–1.87 Ma, and 2.53–2.76 Ma, respectively (Gradstein et al., 2012).

Since the Late Pleistocene, three large-scale transgressions have occurred, and the highest global sea level took place in the MIS5 stage in eastern China (Liu et al., 2009, 2010; Wang et al., 2013). The OSL ages at 39.00–39.20 m, 32.70–32.90 m, and 26.20–26.40 m are 166.58 ± 4.14 ka, 158.48 ± 12.89 ka, and 153.65 ± 16.56 ka, respectively. The measured ages based on OSL techniques may overestimate the actual values in marine sediments due to incomplete sunlight bleaching during OSL analysis (Jacobs, 2008).

The AMS^{14}C ages at 10.90 m, 12.50 m, and 14.50 m are 25,807 ± 159 cal a BP, 38,919 ± 578 cal a BP, and 30,329.5 ± 416 cal a BP, respectively, which indicate that the formation of DU3 occurred during the MIS3. Old carbon mixed in with the tested organic matter may

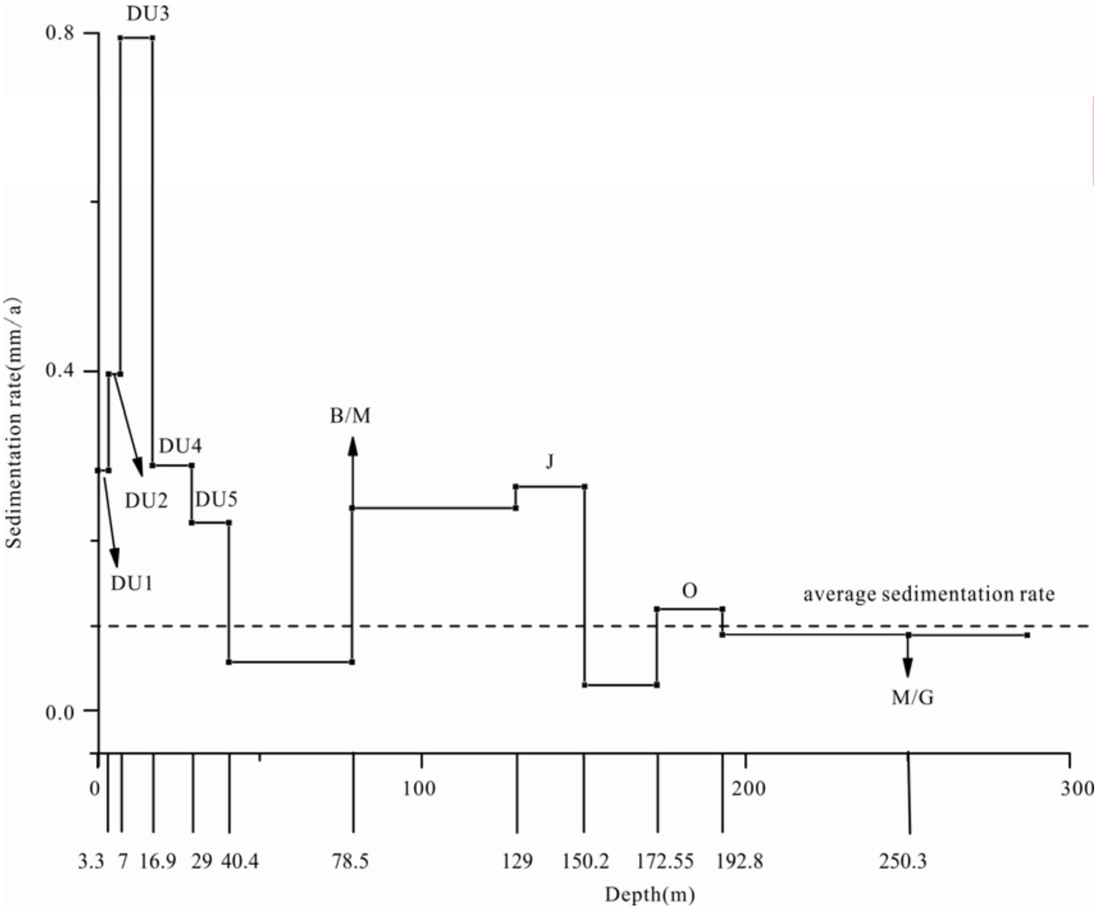

Fig. 6. Age-depth model of the TZK9 core based on magnetostratigraphy, OSL, and AMS^{14}C techniques.

explain why the age at 12.50 m was older than that at 14.50 m. The sedimentation rate during the MIS3 in Fig. 6 was the average age between the 25,807 ± 159 cal a BP date at 10.90 m and the 30,329.5 ± 416 cal a BP date at 14.50 m.

It has been shown in some studies that the age of the second and first hard clay layers in the Subei Basin is MIS4 and 12–25 cal ka BP (Chen Qingqiang and Li Congxian, 1998). The first hard clay layer marks the boundary between the Holocene and the Pleistocene (Chen Baozhang et al., 1991; Deng Bing et al., 1999, 2004). The Subei Basin experienced a large-scale transgression in the Holocene (Ling Shen, 2001; Guo Shengqiao et al., 2013; Zhu Cheng et al., 2016). Therefore, DU5 (29.00–40.40 m), DU4 (16.90–29.00 m), DU3 (7.00–16.90 m), DU2 (3.33–7.00 m), and DU1 (0.00–3.33 m) correspond to the MIS5, MIS4, MIS3, MIS2, and MIS1, respectively.

The B/M boundary and the base of the Late Pleistocene are located at 78.50 and 40.40 m, respectively, which indicates that the sedimentation rate during the Middle Pleistocene was 0.058 mm/a. The 0.25–0.27 Ma age for DU7 (45.50–48.20 m) and the 0.126–0.21 Ma age for DU6 (40.40–45.50 m) correspond to the MIS7 and MIS6, respectively, and the sections of 70.50–71.10 m, 64.80 m, 60.30–61.20 m, 57.05–58.50 m, and 51.80–53.70 m correspond to ages of 0.64–0.65 Ma, 0.54 Ma, 0.47–0.48 Ma, 0.41–0.44 Ma, and 0.32–0.35 Ma, respectively, using linear interpolation.

5.2 Sedimentary history and marine transgressions since ~3.00 Ma

(1) DU9 (3.00–1.01 Ma). The average deposition rate was 0.095 mm/a (286.86 m/3.00 Ma) since the late Pliocene, while the average sedimentation rate since the Middle Pleistocene has remained near 0.01 mm/a (78.50 m/0.78 Ma) (Fig. 6). These rates indicate that the sedimentary environment has been relatively stable and that stratigraphy was relatively continuous in the Subei Basin during the Quaternary. The sedimentary environment was continental with an absence of foraminifera, and the environment was characterized by riverbeds with strong hydrodynamic forces and floodplains with weak water power. The ages of the sandy gravel, that is, 1.01–1.04 Ma (134.60–144.10 m), 1.77–1.87 Ma (171.50–183.50 m), and 2.53–2.76 Ma (245.90–267.80 m), are consistent with the ages of the uplift of the Tibetan Plateau (2.5, 1.7, and 1.1 Ma, respectively) (Li Jijun and Fang Xiaomin, 1999). The uplift of the Tibetan Plateau caused the subsidence of eastern Chinese basins (Pang Yumao et al., 2017), increased of rivers' longitudinal, enhanced hydrodynamic forces, and formed sandy gravel and its unconformable contact with underlying clays. Therefore, tectonic subsidence had a dominant influence on the development of riverbeds.

(2) DU8 (1.01–0.27 Ma). This unit contains fluvial facies and six sea-level high stands. The first high stand is traceable back to between 0.83 and 0.84 Ma, which is based on the appearance of shell sand and horizontal bedding in the core that was affected by tidal action. Other sea-level high stands occurred during the following periods: 0.64–0.65 Ma, 0.54 Ma, 0.47–0.48 Ma, 0.41–0.44 Ma, and 0.32–0.35 Ma.

There were three small-scale transgressions that occurred in the South Yellow Sea at ~1.66 Ma, ~1.44 Ma, and ~1.03 Ma in the Early Pleistocene (Liu et al., 2016a). The first transgression began at 1.66 Ma due to regional subsidence caused by the Zhe-Min Uplift (Liu et al., 2018). However, minor subsidence from the uplift of the Miaodao Islands, at ~0.83 Ma, caused the first transgression along the west coast of the Bohai Sea (Liu et al., 2016b). A sea-level high stand was detected at the TZK9 core site, which shows that the Subei Basin may have subsided to some degree and then experienced rapid subsidence between 0.83 Ma and 0.84 Ma.

Evidence was found for the occurrence of 10 transgressions in the BH08 core in the southern Bohai Sea during the Middle–Early Pleistocene. The ages of these transgressions correspond to the interglacial period during MIS 7 to MIS 25. The earliest occurred at 0.95 Ma since 1 Ma (Li Xiaoyan et al., 2015). A large number of foraminifera were found in the 144.40–145.10 m (1.12–1.13 Ma), 109.10–119.20 m (0.9–0.96 Ma), 90.10–94.30 m (0.82–0.83 Ma), 76.21 m, and 57.81 m intervals of the XH-2 core in the Subei Basin (Zhang Maoheng et al., 2009).

The first transgression age, sea-level high stand, and the transgressions in the Early–Middle Pleistocene vary throughout eastern China. In previous studies, the transgression ages have been calculated by linear interpolation on the basis of the polarity reversal boundary age of the magnetic strata (Cheng Yu et al., 2016; Liu et al., 2016a, 2016b, 2018) or using the astronomical rhythms method (Yi et al., 2012, 2015; Yao et al., 2014). However, continuous sediment stratigraphy is a requirement to use the previously mentioned methods. Different from loess, deep-sea sediments, and ice cores of the world, there are a number of occurrences of developed erosional surfaces in the sediment, which caused discontinuous strata. In addition, the riverbed deposition rates are significantly different from the floodplain deposition rates. The reasons for these discrepancies may have led to the diversity between the ages obtained by linear interpolation (or astronomical rhythms) and the actual values.

Since the Late Pliocene, the paleotopography of the Subei Basin has been quite different from that of the South Yellow Sea Basin (Table 3 and Fig. 7). The paleotopography gradually decreased from the west to the east during the Early–Middle Pleistocene. The paleotopography decided whether the observed area affected by oceanic actions, especially by weak-intensity and small-scale transgressions. Transgression affects low-lying areas, whereas elevated areas maintain a terrestrial signature. During the same period, multiple facies formed when the sea-level rise was insignificant (Zhu Cheng et al., 2016). Therefore, due to a lack of absolute age control and differences in paleotopography, the timing of the first transgression and transgressions in the Early–Middle Pleistocene were different when compared with other cores from eastern China.

DU7–DU1 (0.25–0.00 Ma). Since 0.25 Ma, the study area has been affected by four large-scale transgressions and three terrestrial depositional events due to the effects of global sea-level change. Due to global warming, glaciers melted and the sea level rose during the MIS7, MIS5, MIS3, and MIS1 periods (Miller et al., 2005), and oceanic and enriched foraminifera covered the study area. These environments were characterized by tidal zones, intertidal zones, and lagoons with relatively weak hydrodynamics. During global cooling, glaciers expanded and the sea level retreated during the MIS6, MIS4, and MIS2 periods, and the study area developed hard clay layers and was a terrestrial environment.

5.3 Regional comparison of large-scale transgressions in the western Subei Basin

The B/M boundary in the TZK9 and XH-2 cores (Zhang Maoheng, 2009) is 78.50 and 80.70 m, respectively, which indicates that the paleotopography has remained flat since the Middle Pleistocene and that transgressive layers are comparable horizontally.

Transgressive layers deposited during the MIS7 were thin and were buried at a depth of 48–52 m. A low abundance of foraminifera was observed at a depth of 45.50–48.20 m in the TZK9 core and at a depth of 44.79–51.11 m in the XH-2 core (Zhang Maoheng, 2009), which indicates that the transgression was weak. The sea level was approximately 20–35 m below the present sea level (bpsl) (Miller et al., 2005), and the Asian summer monsoon was strong (Guo et al., 1998) during the MIS7 period. The seawater covered the western Subei Basin, where lagoon facies formed with dominant dark-gray clay.

The transgressive strata that formed in the MIS5 period are 5–12 m thick and are buried at a depth of 35–41 m. A large number of foraminifera (25–423 pieces/50 g) were found at 29.00–40.4 0m and 30.58–36.81 m in the TZK9 and XH-2 cores (Zhang Maoheng, 2009), respectively, which indicates that the transgression was strong and widespread. The highest sea level during the MIS5 was 25 m above present levels (Miller et al., 2005). The study area was covered by seawater in an intertidal and tidal plain and gray clayey silt and silt–clay couplets with horizontal bedding formed.

The transgressive strata formed during the MIS3 are buried at a depth of 16–23 m. Abundant foraminifera (40–830 pieces/50 g) were slightly larger than that of the MIS5 and were observed at depths of 7.00–16.90 m in the TZK9 core and 13.30–22.50 m in the XH-2 core (Zhang Maoheng, 2009). However, there were no significant differences in the thickness of strata between the two periods, which indicates that the transgression strength was comparable.

Strata in the Holocene were buried at a depth of 2–4 m. A small number of foraminifera with small bodies were found at a depth of 0.00–3.33 m in the TZK9 core, which suggests that this transgression was weak and that the

Table 3 Details of the sediment cores from the Subei Basin and the South Yellow Sea

Core No.	Latitude	Longitude	Elevation (m)	Core length (m)	B/M (m)	M/G (m)	Source
TZK9	32°35′ N	120°6′ E	2	286.86	78.5	250.3	This study
BY1	33°14′ 21″ N	119°22′41″ E	5	96.81	39.16	95.22	Yang Jinghong et al. (2006)
XH-1	32°44′ 0″ N	119°53′26″ E	2	350.08	86.5	286.18	Shu Qiang (2004)
XH-2	32°44′ 31″ N	119°53′56″ E	2	743.11	80.7	284.5	Zhang Maoheng (2009)
NHH01	35°13′ N	123°13′ E	−73	125.64	68.4	101.54	Liu et al. (2014a)
CSDP-1	34°18′ N	122°22′ E	−52.5	300.1	73.68	227.16	Liu et al. (2016a)

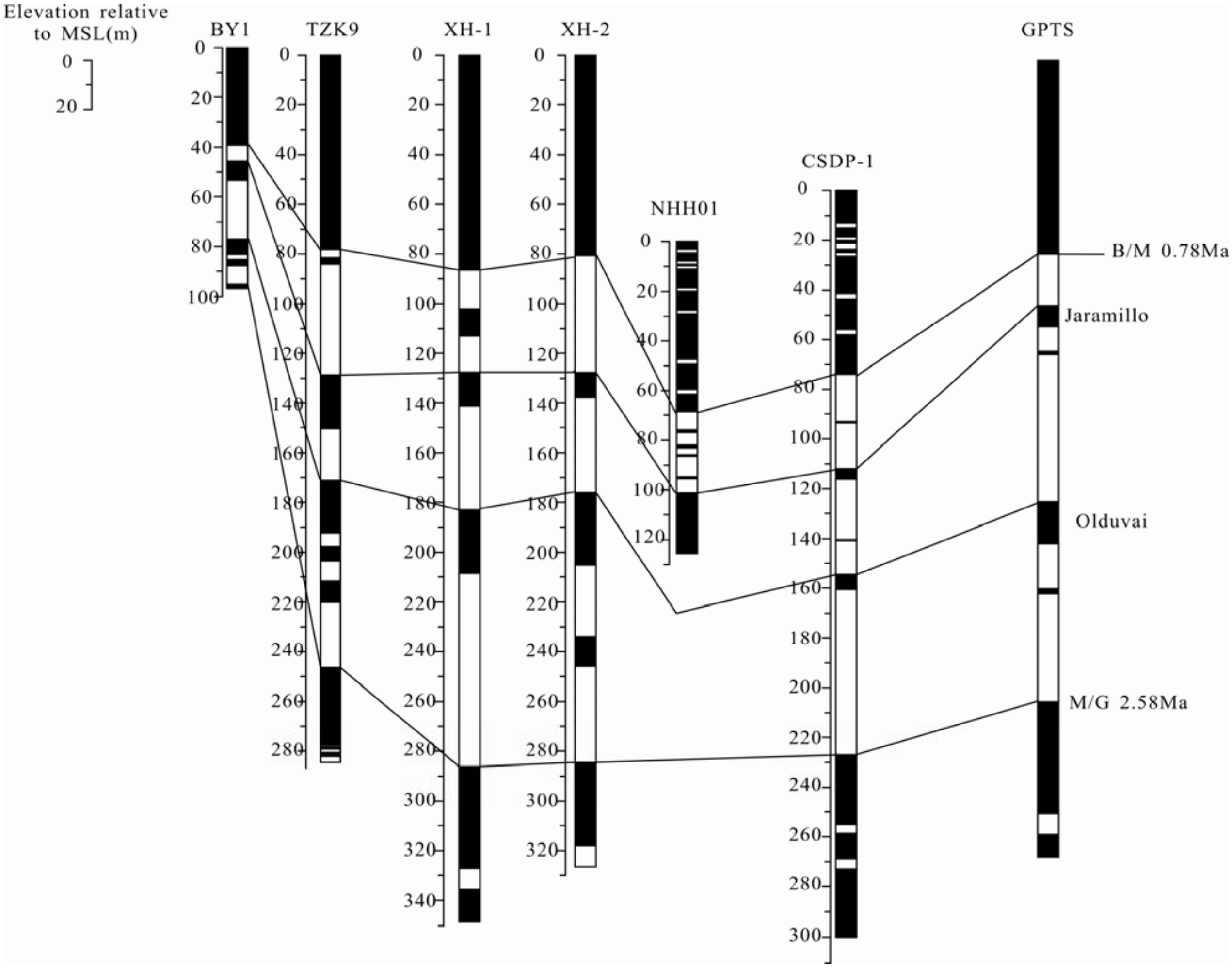

Fig. 7. Magnetostratigraphy of the long core from the Subei Basin and South Yellow Sea.
Data source: BY1 (Yang Jinghong et al., 2006), XH-1 (Shu Qiang, 2004), XH-2 (Zhang Maoheng, 2009), NHH01 (Liu et al., 2014a), CSDP-1 (Liu et al., 2016a), and the Geomagnetic Polarity Timescale (GPTS; Gradstein et al., 2012). All core elevations are relative to contemporary mean sea-level (MSL). The black and white intervals represent normal and reversed polarities, respectively.

environment was a lagoon.

Therefore, the transgression strength of DU5 was identical to that of DU3, both were higher than DU7, and DU1 was the weakest in the western part of the Subei Basin. These results are quite different from the height of global sea level, which is thought to be MIS5 > MIS1 > MIS7 > MIS3.

The calculated average sedimentation rate based on the 200–300 m interval of strata is 0.077–0.116 mm/a (Wu Biaoyun and Li Congxian, 1987; Cheng Yu et al., 2016, 2018b; Liu et al., 2016a) during the Quaternary in eastern China. Subsidence for the MIS3 period was approximately 4–6 m according to this rate. Therefore, the sea level recorded in the TZK9 core during the MIS3 ranged from approximately 35 to 0 m bpsl on the basis of structural corrections (approximately 4–6 m), ground elevation (2 m), and sea level (approximately 0–20 m bpsl) estimated by foraminiferal assemblages (Wang Pinxian et al., 1985, 1988).

Global ice sheets mainly controlled the global sea level during the MIS3, which was approximately 40-85 m bpsl (Imbrie et al., 1984; Shackleton et al., 1987; Chappell et al., 1996). However, the regional sea level recorded in the transgressive formations was between approximately 5 and 35m bpsl in eastern China (Emery et al., 1971; Wang Jingtai and Wang Pinxian, 1980; Yang Dayuan et al., 2004; Zhang Zhenke et al., 2010; Sun et al., 2015; Yu Ge et al., 2016). The regional sea-level change is affected not only by the global sea-level change, but also by multiple sea–land lifting (Wang et al., 2013; Yu Ge et al., 2016), glacial isostatic adjustment (Yu et al., 2007), and sediment compaction (subsidence) (Edwards et al., 2000).

A large-scale transgression occurred during the Holocene in eastern China, which affected the Yangtze River Delta and the majority of the Subei Basin. The Yangtze River Delta experienced the largest transgression since the Late Pleistocene (Zhao et al., 2018), whereas the intensities of simultaneous transgressions were weak as interpreted by lagoon records in the Subei Basin (Zhu Cheng et al., 2016). The reason for this phenomenon is the development of a shell ridge (Zhu Cheng et al., 2016) and sand dams in the Yangtze River (Song et al., 2013; Cheng Yu et al., 2018a).

6 Conclusions

(1) Fluvial facies dominated the sedimentary environment from 3.00 to 1.01 Ma. There were occurrences of fluvial facies and several sea-level high stands between 1.01 and 0.25 Ma, of which the first high stand is traceable back to 0.83–0.84 Ma. Due to the lack of absolute age control and differences in paleotopography, the timing of the first transgression and the transgressions in the Early–Middle Pleistocene are different from other cores drilled in eastern China.

(2) The study area has been affected by four large-scale transgressions since 0.25 Ma. The four marine sedimentary layers, known as DU7 (buried at a depth of 48–52 m), DU5 (buried at a depth of 35–41 m), DU3 (buried at a depth of 16–23 m), and DU1 (buried at a depth of 2–4 m), correspond to the MIS7 (210–250 ka), MIS5, MIS3, and Holocene, respectively.

(3) The transgression strength of the DU5 was identical to that of the DU3, both were higher than DU7, and DU1 was the weakest. The various transgression strengths reflect global sea-level changes, tectonic subsidence, shell ridges, and sand dams.

(4) Both local tectonics and global sea level drove the evolution of sedimentation and transgressions in the Subei Basin.

Acknowledgments

This study was jointly supported by the China Geological Survey Project (DD20160060, 121201140 42901) and the National Natural Science Foundation of China (41502119, 41371207).

Manuscript received July 6, 2018
accepted Sept. 13, 2018
associate EIC HAO Ziguo
edited by LIU Lian

References

Chappell, J., Omura, A., Esat, T., McCulloch, M., Pandolfi, J., Ota, Y., and Pillans, B., 1996. Reconciliaion of late Quaternary sea levels derived from coral terraces at Huon Peninsula with deep sea oxygen isotope records. *Earth and planetary science letters*, 141(1–4): 227–236.

Chen Baozhang, Li Congxian and Ye Zhizheng, 1991. Holocene bottom boundary and hard clay band in the northern flank of the Changjiang river delta. *Marine geology & Quaternary geology*, 11(2): 37–46 (in Chinese with English abstract).

Chen Qingqiang and Li Congxian, 1998. Studies on origin of the late Pleistocene stiff clays at Yangtze delta. *Scientia Geographica Sinica*, 18(1): 53–57 (in Chinese with English abstract).

Chen Wanli, Gu Hongqun and Zhang Daozhegn., 1998. Quaternary transgression and coastal changes in Jiangsu Province. *Geology of Jiangsu Province*, 22(Suppl.): 45–50 (in Chinese).

Cheng Yu, Li Xiangqian, Zhao Zengyu, Zhang, Xiangyun and Guo Gang, 2016. Magnetostratigraphy and heavy minerals records of Core TZK9 in Subei Basin. *Journal of Geomechanics*, 22(4): 994–1003 (in Chinese with English abstract).

Cheng Yu, Li Xiangqian, Shu Junwu, Zhao Zengyu, Zhang Xiangyun and Guo Gang, 2018a. The formation and evolution of the Changjiang River delta since Last Glacial. *Quaternary Science*, 38(3): 746–755 (in Chinese with English abstract).

Cheng Yu, Li Xiangqian, Zhao Zengyu, Zhang Xiangyun and Guo Gang. 2018b. Detrital Zircon U–Pb ages and its provenance significance in the TZK3 core from the Yangtze River delta, *Journal of Geomechanic*, 24(5): 635–644 (in Chinese with English abstract).

Deng Bing and Li Congxian, 1999. Paleoclimate recorded in the first layer of paleosoil in Yangtze delta area. *Marine Geology & Quaternary Geology*, 19(3): 29–37 (in Chinese with English abstract).

Deng Bing, Li Congxian, Zhang Jing and Wu Guoxuan, 2004. Correlation of paleosol development in the Changjiang delta with sea level fluctuations in the late Pleistocene. *Quaternary Sciences*, 24(2): 222–230 (in Chinese with English abstract).

Duan Liu'an, Gui Huangling and Yang Xiaoyong. 2017. Geological and Geochemical Constraints on the Newly Discovered Yangchongli Gold Deposit in Tongling Region, Lower Yangtze Metallogenic Belt. *Acta Geologica Sinica* (English Edition), 91(6): 2078–2108.

Duan, Z.Q., Liu, Q.S, Shi, X.F, Yao, Z.Q, Liu, J.X, and Su, K., 2015. Reconstruction of high–resolution magnetostratigraphy of the Changjiang (Yangtze) River Delta, China. *Geophysical Journal International*, 204(2): 948–960.

Edwards, R.J., and Horton, B.P., 2000. Reconstructing relative sea–level change using UK salt–marsh foraminifera. *Marine Geology*, 169(1): 41–56.

Emery, K.O., 1971. Post–Pleistocene levels of East China Sea. *Late Cenozoic glacial ages*: 381–390.

Friedman, G.M., and Sanders, J.E., 1978. Principles of sedimentology. New York, Wiley: 1–792.

Ge Shulan, Shi Xuefa, Zhu Rixiang, Liu Yanguang, Yin Ping and Liu Lejun, 2005. Magnetostratigraphy of borehole EY02–2 in the southern Yellow Sea and its paleoenvironmental significance. *Chinese Science Bulletin*, 50(22): 2531–2540 (in Chinese).

Gradstein, F.M., Ogg, J.G., Schmitz, M.D., and Ogg, G.M., 2012. The Geologic Time Scale 2012. Elsevier, U. K.

Guo, Z.T., Liu, T.S., Fedoroff, N., Wei, L.Y., Ding, Z.L., Wu, N.Q., Lu, H.Y., Jiang, W.Y., and An, Z.S., 1998. Climate extremes in loess of China coupled with the strength of deep–water formation in the North Atlantic. *Global and Planetary Change*, 18(3–4): 113–128.

Guo Shengqiao, Ma Qiubing, Zhang Xiangyun, Ge Yun and Gong Xunlong, 2013. Holocene environmental changes in Lixiahe area. *Geology in China*, 40(1): 341–351 (in Chinese with English abstract).

Imbrie, J., Hays, J.D., Martinson, D.G., McIntype, A., Mix, A.C., Morley, J.J., Pisias, N.G., Prell, W.L., and Shackleton, N.J., 1984. The orbital theory of Pleistocene climate, support from a revised chronology of the marine d18O record. Berger A. Milankovitch and Climate. New York, Reidel Pub. Company: 269–305.

Jacobs, Z., 2008. Luminescence chronologies for coastal and marine sediments. *Boreas*, 37(4): 508–535.

Li Jijun and Fang Xiaomin, 1999. Uplift of Qinghai–Tibetan Plateau and environmental change. *Chinese Science Bulletin*, 44(23): 2217–2224.

Li Xiaoyan, Zhao Quankong, Yao Zhenquan, Wang Qiang, Jian Zhimin and Shi Xuefa, 2015. Transgressive records of last million years in the Bohai Sea, China, evidence from foraminifera and ostracoda of core BH08. *Marine Geology & Quaternary Geology*, 35(6): 93–108 (in Chinese with English abstract).

Li Shoujun, Gui Xiaohui, Xu Hua, Zhang Zhuo, Zhao Xiuli, Liu, Qiang and Liu Xiao, 2016. Distribution charcteristics of ostracods and evolution of the sedimentary environment of the late Quaternary in the Laizhou Bay, Bohai Sea. *Quaternary Sciences*, 36(6): 1475–1488 (in Chinese with English abstract).

Li Xiang, Li Rihui, Chen, Xiaohui, Qiang Xiaoke and Zhao Hui, 2016. Quaternary magnetostratigraphy records in the sediments of core TJC–1 in the western Bohai Sea. *Quaternary Sciences*, 36(1): 208–215 (in Chinese with English abstract).

Li Shoujun, Gui Xiaohui, Xu Hua, Zhang Zhuo, Zhao Xiuli, Gao Zongjun, Liu Qiang and Liu Xiao. 2017. Distribution characteristics of benthic foraminifera of the late Quaternary in Laizhou bay, Bohai Sea, China and its paleoenvironmental significance. *Acta Geologica Sinica*, 91(2): 287–301 (in Chinese with English abstract).

Lin Jingxing. 1977. Preliminary notes on Quaternary transgressions and regressions in N. China Plain. *Acta Geologica Sinica*, (2): 11–18 (in Chinese with English abstract).

Lin, J.X., Zhang, S.L., Qiu, J.B., and Wu, B.Y., 1989. Quaternary marine transgressions and paleoclimate in the Yangtze River delta region. *Quaternary Research*, 32(3): 296–306.

Lin, J.X., Dai, L.P., Wang, Y., and Min, L., 2012. Quaternary marine transgressions in eastern China. *Journal of Palaeogeography*, 1(2): 105–125.

Liu, J., Saito, Y., Wang, H., Zhou, L.Y., and Yang, Z.G., 2009. Stratigraphic development during the late Pleistocene and Holocene offshore of the Yellow River delta, Bohai Sea. *Journal of Asian Earth Scien*ces, 36(4–5): 318–331.

Liu, J., Saito, Y., Kong, X.H., Wang, H., Wen, Z.G., and Nakashima, R., 2010. Delta development and channel incision during marine isotope stages 3 and 2 in the western South Yellow Sea. *Marine Geology*, 278(1–4): 54–76.

Liu, J.X., Shi, X.F., Liu, Q.S., Ge, S.L., Liu, Y.G., Yao, Z.Q., Zhao, Q.H., Jin, C.S., Jiang, Z.X., Liu, S.F., Qiao, S.Q., Li, X.Y., Li, C. S., and Wang, C.J., 2014a. Magnetostratigraphy of a greigite - bearing core from the South Yellow Sea, Implications for remagnetization and sedimentation. *Journal of Geophysical Research, Solid Earth*, 119(10): 7425–7441.

Liu, J.X., Shi, X.F., Ge, S.L., Liu, Q.S., Yao, Z.Q., and Yang, G., 2014b. Identification of the thick–layer greigite in sediments of the South Yellow Sea and its geological significances. *Chinese science bulletin*, 59(22): 2764–2775.

Liu, J.X., Liu, Q.S., Zhang, X.H., Liu, J., Wu, Z.Q., Mei, X., Shi, X.F., and Zhao, Q.H., 2016a. Magnetostratigraphy of a long Quaternary sediment core in the South Yellow Sea. *Quaternary Science Reviews*, 144: 1–15.

Liu, J., Wang, H., Wang, F.F., Qiu, J.D., Saito, Y., Lu, J.F., Zhou, L.Y., Xu, G., Du, X.L., and Chen, Q., 2016b. Sedimentary evolution during the last ~1.9 Ma near the western margin of the modern Bohai Sea. *Palaeogeography, Palaeoclimatology, Palaeoecology*, 451: 84–96.

Liu, J., Zhang, X., Mei, X., Zhao, Q.H., Guo, X.W., Zhao, W.N., Liu, J.X., Satio, Y., Wu, Z.Q., Li, J., Zhu, X.Q., and Chu, H.X., 2018. The sedimentary succession of the last ~ 3.50 Myr in the western south Yellow Sea, Paleoenvironmental and tectonic implications. *Marine Geology*, 399: 47–65.

Ling Shen, 2001. Palaeographic changes of the Lixiahe district since the Holocene. *Scientia Geographica Sinica*, 21(5): 474–479 (in Chinese with English abstract).

Lu, H.Y., and An, Z.S., 1997. Pretreatment methods in loess–paleosol granulometry. *Chinese Science Bulletin*, 42: 237–240.

Lu Huayu, Miao Xiaodong and Sun Youbin, 2002. Pretreatment methods and their influences on grain–size measurement of aeolian "red clay" in north China. *Marine Geology & Quaternary Geology*, 22(3): 129–135 (in Chinese with English abstract).

Mei Mingxiang and Liu Shaofeng, 2017. The Late Triassic Sequence-Stratigraphic Framework of the Upper Yangtze Region, South China. *Acta Geologica Sinica* (English Edition), 91(1): 51–75.

Mei, X., Li, R.H., Zhang, X.H., Liu, Q.S., Liu, J.X., Wang, Z.B., Lan, X.H., Liu, J., and Sun, R.T., 2016. Evolution of the Yellow Sea warm current and the Yellow Sea cold water mass since the Middle Pleistocene. *Palaeogeography, Palaeoclimatology, Palaeoecology*, 442: 48–60.

Miller, K.G., Kominz, M.A., Browning, J.V., Wright, J.D., Mountain, G.S., Katz, M.E., Sugarman, P.J., Cramer, B.S., Blick, N.C., and Pekar, S.F., 2005. The Phanerozoic record of global sea–level change. *Science*, 310(5752): 1293–1298.

Pang Yumao, Zhang Xunhua, Xiao Guolin, Guo Xingwei, Wen Zhenhe, Wu Zhiqing and Zhu Xiaoqing, 2017. Characteristics of Meso–Cenozoic Igneous Complexes in the South Yellow Sea Basin, Lower Yangtze Craton of Eastern China and the Tectonic Setting. *Acta Geologica Sinica* (English Edition), 91 (3):971–987.

Shackleton, N.J., 1987. Oxygen isotopes, ice volume and sea level. *Quaternary Science Reviews*, 6(3): 183–190.

Shang Zhiwen, Chen Yongsheng, Jiang Xingyu, Wang Fu, Li Jianfen, Shi Peixin and Wang Hong. 2015. New discovery of a fishing site during Western Han Dynasty and an enlightenment for the "Western Han Dynasty's Transgression" on the west coast of Bohai Bay. Geological review, 61(6): 1468–1481 (in Chinese with English abstract).

Shi Linfeng, Zhai Zhimei, Wang Qiang, Zhang Xuebing and Yang Zhenyu, 2009. Geochronological study on transgression layers of the CQJ4 borehole at Dagang area in Tianjin, China. *Geological Review*, 55(3): 375–384 (in Chinese with English abstract).

Shu Qiang. 2004. Study on the changes of oalaeoenvironment and palaeoclimate during the past 3Ma recorded in Xinghua core ay Northern Jiangsu Basin. Doctoral Dissertation. Nanjing, Nanjing Normal University (in Chinese with English abstract).

Shu Qiang, Li Jijun, Zhao Zhijun, Chen Ye and Zhang Maoheng, 2006. A correlation between magnetic susceptibility and the content of different grain sizes of XH–1#Core in North Jiangsu basin and its significance. *Acta Sedimentologica Sinica*. 24(2): 276–281 (in Chinese with English abstract).

Song, B., Li, Z., Saito, Y., Okuho, J., Li, Z., Lu, A. Q., Hua, D., Li, J., Li, Y. X., and Nakashima, R., 2013. Initiation of the Changjiang (Yangtze) delta and its response to the mid–Holocene sea level change. *Palaeogeography, Palaeoclimatology, Palaeoecology*, 388: 81–97.

Stuiver, M. and Reimer, P. J., 1986–2014. Calib Radiocarbon Calibration Program.

Sun, Z., Li, G., and Yin, Y., 2015. The Yangtze River deposition in southern Yellow Sea during Marine Oxygen Isotope Stage 3 and its implications for sea–level changes. *Quaternary Research*, 83(1): 204–215.

Wang Jingtai and Wang Pinxian, 1980. Relationship between sea–level changes and climatic fluctuations in east China since late Pleistocene. *Acta Geographica Sinica*, 35(4): 299–312 (in Chinese with English abstract).

Wang Pinxian, Min Qiubao, Bian Yunhua and Cheng Xinrong, 1981. Strata of Quaternary transgressions in East China, a preliminary. *Acta Geologica Sinica*, (1): 3–15 (in Chinese with English abstract).

Wang Pinxian, Min Qiubao and Bian Yunhua, 1985. Distribution of Foraminifera and ostracoda in Bottom Sediments of the Northwestern Part of the South Huanghai (Yellow) Sea and its Geological Significance. In: Wang, P, et al. Eds). Marine Micropaleontology of China. Beijing, China Ocean Press: 93–114 (in Chinese).

Wang Pingxian, Zhang Jijun and Zhao Quan, 1988. Distribution of Foraminifera and ostracoda in sediments of the East China Sea (in Chinese). Beijing, China Ocean Press: 1–325.

Wang Qiang and Li Fenglin, 1983. The Chinese of marine–continental conditions in the west coast of the Bohai Gulf during Quaternary. *Marine Geology & Quaternary Geology*, 3

(4): 85–91 (in Chinese with English abstract).
Wang Qiang, Li Fenglin, Li Yude and Gao Xiulin, 1986. Discussion on the naming of Quaternary transgressions in west–southern coast plain of Bohai Sea. *Acta Oceanologica Sinica*, 6(1): 104–115 (in Chinese).
Wang Ying, Zhang Zhenke, Zhu Dakun, Yang Jinghong, Mao Longjiang and Li Shuheng, 2006. River–sea interaction and the north Jiangsu Plain formation. *Quaternary Sciences*, 26 (3): 301–320 (in Chinese with English abstract).
Wang Zhanghua, Qiu Jinbo, Ran Lihua, Yan Xuexin and Li Xiao, 2004. Chronostratigraphy and transgression/regression during late Pleistocene in the southern Changjiang (Yangtze) river delta plain. *Marine Geology & Quaternary Geology*, 24 (4): 1–8 (in Chinese with English abstract).
Wang Zhanghua, Zhao Baocheng, Chen Jing and Li Xiao, 2008. Chronostratigraphy and two transgressions during the late Quaternary in Changjiang delta area. *Journal of Palaeogeography*, 10(1): 99–110 (in Chinese with English abstract).
Wang, Z.H., Jones, B.G., Chen, T., Zhao, B.C., and Zhan, Q., 2013. A raised OIS 3 sea level recorded in coastal sediments, southern Changjiang delta plain, China. *Quaternary Research*, 79(3): 424–438.
Wu Biaoyun and Li Congxian, 1987. Quaternary Geology of the Changjiang Delta. Beijing, China Ocean Press: 1–157 (in Chinese).
Yang Zhigeng, 1993. The sedimentary sequence and palaeogeographic changes of the South Yellow Sea since the Olduvai subchron. *Acta Geologica Sinica*, 67(4): 357–366 (in Chinese with English abstract).
Yang Dayuan, Chen Kefeng and Shu Xiaomin, 2004. A Preliminary study on the paleoenvironment during MIS3 in the Changjiang delta region. *Quaternary Sciences*, 24(5): 525 –530 (in Chinese with English abstract).
Yang Jinghong, Wang Yin, Zhang Zhenke, Guilbault J P, Mao Longjiang, Wei Ling, Guo Wei, Li Shuheng, Xu Jun and Ji Xiaomei, 2006. Major element records of land–sea interaction and evolution in the past 2.58 Ma from the Baoying borehole sediments, Northern Jiangsu plain, China. *Quaternary Sciences*, 26(5): 340–352 (in Chinese with English abstract).
Yang Jinghong, Wang Ying, Zhang Zhenke, Guilbault J P, Mao Longjiang, Wei Ling, Guo Wei, Li Shuheng, Xu Jun and Ji Xiaomei, 2007. Geochemical characteristics of trace elements in Baoying borehole sediments and their implications for depositional environments. *Quaternary Sciences*, 27(5): 735–749 (in Chinese with English abstract).
Yao, Z.Q., Shi, X.F., Liu, Q.S., Liu, Y.Q., Larrasoafia, J.C., Liu, J.X., Ge, S.L., Wang, K.S., Qiao, S.Q., Li, X.Y., Shi, F.D., Fang, X.S., Yu, Y.G., Yang, G., and Duan, Z.Q., 2014. Paleomagnetic and astronomical dating of sediment core BH08 from the Bohai Sea, China, Implications for glacial–interglacial sedimentation. *Palaeogeography Palaeoclimatology Palaeoecology*, 393: 90–101.
Yi, L., Yu, H.J., Ortiz, J.D., Xu, X.Y., Chen, S.L., Ge, J.Y., Hao, Q.Z., Yao, J., Shi, X.F., and Peng, S.Z., 2012. Late Quaternary linkage of sedimentary records to three astronomical rhythms and the Asian monsoon, inferred from a coastal borehole. *Palaeogeography, Palaeoclimatology, Palaeoecology*, 329: 101–117.
Yi, L., Deng, C.L., Xu, X.Y., Yu, H.J., Qiang, X.K., Jiang, X.Y., Chen, Y.P., Su, Q., Chen, G.Q., Li, P., Ge, J.Y., and Li, Y., 2015. Paleo–megalake termination in the Quaternary, Paleomagnetic and water–level evidence from south Bohai Sea, China. *Sedimentary Geology*, 319(1): 1–12.
Yu Ge, Ye Liangtao, Liao Mengna, Wang Longshen and Li Yongfei, 2016. Quantitative reconstruction, simulation and mechanism study on the late Pleistocene marine transgressions in the coastal plains of China. *Quaternary Science*, 36(3): 711–721 (in Chinese with English abstract).
Yu, S.Y., Berglund, B.E, Sandgren, P., and Lambeck, K., 2007. Evidence for a rapid sea–level rise 7600 yr ago. *Geology*, 351 (3): 891–894.
Yu Zhangxin, Zhang Ke, Li Xiaoyang, Hao Liang and Li Zhongyuan, 2017. The Age of the Old Transgression Sequence in the Pearl River Delta, China. *Acta Geologica Sinica* (English Edition), 91(4): 1515–1516.
Zhang Hucai, Wang Qiang, Peng Jinlan and Chen Guangjie, 2008. Ostracod assemblages and their paleoenvironmental significance from shell bar section of paleolake Qarhan, Qaidam Basin. *Quaternary Sciences*, 28(1): 103–111 (in Chinese with English abstract).
Zhang Maoheng, 2009. Sedimentary infilling and environmental changes of the northern Jiangsu Basin since latest Miocene recorded in Xinghua cores. Doctoral Dissertation. Nanjing, Nanjing Normal University (in Chinese with English abstract).
Zhang Zhenke, Xie Li, Zhang Yunfeng, Xu Jun, Li Shunheng and Wang Ying, 2010. Sedimentary records of the MIS3 transgression event in the borth Jiangsu plain, China. *Quaternary Sciences*, 30(5): 883–891 (in Chinese with English abstract).
Zhao, B.C., Yan, X.X., Wang, Z.H., Shi, Y.J., Chen, Z.Y., Xie, J.L., Chen, J., He, Z.F., Zhan, Q., and Li, X., 2018. Sedimentary evolution of the Yangtze River mouth (East China Sea) over the past 19,000 years, with emphasis on the Holocene variations in coastal currents. *Palaeogeography Palaeoclimatology Palaeoecology*, 490: 431–449.
Zhao Songling, Yang Guanghu, Cang Shuxi, Zhang Hongcai, Huang Qinfu, Xia Dongxing, Wang Yongjie, Liu Fushou and Liu Chengfu, 1978. On the marine stratigraphy and coastlines of the western coast of the gulf of Bohai. *Oceanologia and Lininologia*, 9(1): 15–25 (in Chinese with English abstract).
Zhu Cheng, Wu Li, Li Lan, Zhao Quanhong, Zhang Wenqing, Li Kaifeng, Li Bing, Tan Yan, Wang Kunhua, Jia Tianjiao, Guo Tianhong, Lin Liugeng, Ding Jinlong, Wang Zhijian and He Hansheng, 2016. Recognition of sea–level change during the Neolithic period in the Jiangsu Area, East China. *Chinese Science Bulletin*, 61(3): 374–387 (in Chinese).

About the first author

CHENG Yu, female, born in 1989 in Nanchong City, Sichuan Province, master; graduated from Institute of Geomechanics, Chinese Academy of Geological Sciences; a engineer of the Institute of Geological Survey of Jiangsu Province. She is now interested in the study on the sedimentary evolution in Yangtze River delta and Subei Basin. Email: ftchengyu @ msn.com; phone: 18751880474.